Author/s:
Yao, S;Meikle, TG;Sethi, A;Separovic, F;Babon, JJ;Keizer, DW

Title:
Measuring translational diffusion of 15N-enriched biomolecules in complex solutions with a simplified 1H-15N HMQC-filtered BEST sequence

Date:
2018-12-01

Citation:
Yao, S., Meikle, T. G., Sethi, A., Separovic, F., Babon, J. J. & Keizer, D. W. (2018). Measuring translational diffusion of 15N-enriched biomolecules in complex solutions with a simplified 1H-15N HMQC-filtered BEST sequence. European Biophysics Journal, 47 (8), pp.891-902. https://doi.org/10.1007/s00249-018-1311-5.

Persistent Link:
https://hdl.handle.net/11343/282910

Measuring Translational Diffusion of ^{15}N-enriched Biomolecules in Complex Solutions with a Simplified ^{1}H-^{15}N HMQC-filtered BEST Sequence

Shenggen Yao[1,*], Thomas G. Meikle[2], Ashish Sethi[1,3], Frances Separovic[1,4], Jeffrey J. Babon[5,6], and David W. Keizer[1]

[1]*Bio21 Molecular Science and Biotechnology Institute, The University of Melbourne, VIC 3010, Australia*

[2]*School of Science, College of Science, Engineering and Health, RMIT University, Melbourne, VIC 3000, Australia*

[3]*Department of Biochemistry & Molecular Biology, The University of Melbourne, VIC 3010, Australia*

[4]*School of Chemistry, The University of Melbourne, VIC 3010, Australia*

[5]*The Walter and Eliza Hall Institute of Medical Research, Parkville, VIC 3052, Australia*

[6]*Department of Medical Biology, The University of Melbourne, VIC 3010, Australia*

* Corresponding author:

Shenggen Yao

Bio21 Molecular Science and Biotechnology Institute

The University of Melbourne

VIC 3010, Australia

Phone: +61 (3) 83442203 Facsimile: +61 (3) 93478265

E-mail: shyao@unimelb.edu.au

Abstract

Pulsed-field gradient nuclear magnetic resonance (PFG-NMR) has seen an increase in applications spanning a broad range of disciplines where molecular translational diffusion properties are of interest. The current study introduces and experimentally evaluates the measurement of translational diffusion coefficients of ^{15}N-enriched biomolecules using a ^{1}H-^{15}N HMQC-filtered band-selective excitation short transient (BEST) sequence as an alternative to the previously described SOFAST-XSTE sequence. The results demonstrate that accurate translational diffusion coefficients of ^{15}N-labelled peptides and proteins can be obtained using this alternative ^{1}H-^{15}N HMQC-filtered BEST sequence which is implementable on NMR spectrometers equipped with probes fitted with a single-axis field gradient, including most cryoprobes dedicated to bio-NMR. The sequence is of potential use for direct quantification of protein or peptide translational diffusion within complex systems, such as in mixtures of macromolecules, crowded solutions, membrane-mimicking media and in bicontinuous cubic phases, where conventional sequences may be not readily applicable due to the presence of intense signals arising from sources other than the protein or peptide under investigation.

Keywords: ^{1}H-^{15}N HMQC BEST; complex solutions; crowded solutions; detergent micelles; isotope-filtered; PFG-NMR; translational diffusion

Introduction

*P*ulsed-*F*ield *G*radient *N*uclear *M*agnetic *R*esonance (PFG-NMR), since it was first demonstrated experimentally in 1960's, has established itself as a powerful means for probing molecular translational diffusion with applications spanning virtually all fields where molecular motion is present. Over the last two decades, translational diffusion of biomolecules probed by PFG-NMR, both in aqueous solution and under crowded conditions (Price 2009) (Wang et al. 2010), has seen an increase in applications for the characterization of biophysical/biological processes involving changes of effective hydrodynamic radii for biomolecules, such as (i) protein or peptide self-association and aggregation (Ali et al. 2006; Altieri et al. 1995; Bocian et al. 2008; Dingley et al. 1995; Jansma et al. 2010; Wahlstrom et al. 2012; Yao et al. 2004; Yao et al. 2000), (ii) protein folding and unfolding (Buevich and Baum 2002; Dehner and Kessler 2005; McLachlan et al. 2007), and (iii) ligand binding and protein-protein interactions (Rothe et al. 2016; Sillerud and Larson 2012; Yan et al. 2002). PFG-NMR has also been applied for the study of *I*ntrinsically *D*isordered *P*roteins (IDP) (Melnikova et al. 2017; Wang et al. 2012; Wu et al. 2008; Yao et al. 2016; Zhang et al. 2008), a unique class of proteins which only adopt stable tertiary structures in the presence of their binding partners (Dyson and Wright 2005). An extensive range of PFG-NMR pulse sequences, developed primarily by extensions and/or modifications to the original forms of *S*pin *E*cho (SE) (Stejskal and Tanner 1965) and *ST*imulated *E*cho (STE) sequences (Tanner 1970) to accommodate ever expanding fields of applications, have been proposed. These include various ^{15}N-edited *H*eteronuclear *S*ingle *Q*uantum *C*oherence (HSQC) or *T*ransverse *R*elaxation-*O*ptimization *S*pectroscop*Y* (TROSY) based sequences dedicated to ^{15}N-enriched biomolecules in solution for studies such as: protein folding (Buevich and Baum 2002), protein backbone amide exchange (Andrec and Prestegard 1997; Brand et al. 2007), translational diffusion in macromolecular assemblies (Horst et al. 2011) and of large protein

complexes (Didenko et al. 2011), slow diffusion of partially disordered protein (Augustyniak et al. 2011), or simply for filtering of polypeptide and protein signals in complex mixtures (Rajagopalan et al. 2004).

The *B*and-selective *E*xcitation *S*hort *T*ransient (BEST) scheme has gained remarkable popularity over the last decade and is adopted in many types of experiments, including a suite of sequences used for conventional backbone chemical shift assignments of proteins (Lescop et al. 2007) and molecular translational diffusion measurements (Augustyniak et al. 2011; Shukla and Dorai 2011; Yao et al. 2014). The BEST sequence achieves significant spectral sensitivity gain through the use of band-selective RF pulses to realize longitudinal relaxation optimization for a sub-group of nuclear spins by avoiding perturbation of magnetizations of other protons not involved in coherence transfer pathways for a specific type of NMR spectroscopy (Schanda 2009; Schanda and Brutscher 2005). In this report, we introduce an alternative ^{1}H-^{15}N *H*eteronuclear *M*ultiple *Q*uantum *C*oherence (HMQC) filtered BEST sequence related to the previously described BEST-XSTE (BEST-heteronuclear stimulated echo experiment) and SOFAST-XSTE (band-Selective Optimized Flip-Angle Short-Transient XSTE) sequences (Augustyniak et al. 2011) for the measurement of ^{15}N-labelled proteins and peptides in complex solutions.

This alternative ^{1}H-^{15}N HMQC-filtered sequence introduced here takes a simpler form than both the BEST-XSTE and SOFAST-XSTE sequences with only a single-axis field gradient employed and is complementary to the previously described 3D BEST ^{1}H-^{13}C HMQC-edited sequence used for resolving spectral overlaps in DOSY (Shukla and Dorai 2011). This alternative sequence, therefore, can be readily implemented on NMR spectrometers equipped with probes fitted with a single-axis field gradient, including most cryoprobes dedicated to biomolecular studies. This alternative sequence provides additional means for direct measurements of ^{15}N-enriched peptides and proteins in complex solution

conditions, such as SDS micelles commonly used to mimic a membrane environment and crowded protein solutions for simulating the in-cell background. The non-selective ^{1}H-^{15}N HSQC-edited (Buevich and Baum 2002; Didenko et al. 2011) or band-selective ^{1}H-^{13}C HMQC edited (Shukla and Dorai 2011) sequences may be not directly applicable under such conditions due to either: (i) the presence of underlying amide solvent exchange, or (ii) intense background signals in the aliphatic region. The sequence was first experimentally evaluated using a phosphopeptide with a single ^{13}C/^{15}N-labelled residue and comparing the translational diffusion coefficient measured with those obtained using alternative sequences, namely (1) conventional *B*ipolar *P*ulse *P*air *L*ongitudinal *E*ddy-current *D*elay (BPP-LED) sequence with water suppression achieved with excitation-sculpting (Figure S1c, Supplemental Materials), (2) the non-isotope-edited BEST-STE sequence (Figure S1b, Supplemental Materials) (Yao et al. 2014), and (3) ^{1}H-^{13}C HMQC-edited BEST sequence (Figure S1a, Supplemental Materials) (Shukla and Dorai 2011). Subsequently, results are presented using the ^{1}H-^{15}N HMQC-filtered BEST sequence for: (1) a uniformly ^{15}N-labelled B1 immunoglobulin-binding domain of Streptococcal protein (GB1) in an imidazole buffer, (2) the phosphopeptide in the presence of equimolar ribonuclease A (RNase A), and (3) a single residue ^{15}N-labelled model membrane protein, gramicidin A, in *S*odium *D*odecyl *S*ulfate (SDS) micelles.

Materials and methods

PFG-NMR diffusion measurements and analyses

All spectra were acquired either on a Bruker Avance III 600 equipped with a TCI or a Bruker Avance II 800 spectrometer equipped with a TXI cryoprobe fitted with a single-axis field gradient (*G*z). The field gradient strengths of both spectrometers were calibrated by back calculation using the self-diffusion coefficient of residual H_2O in a 100% $^{2}H_2O$ sample

118 measured at 298.13 K against published value of 1.90 x 10^{-9} m^2 s^{-1} (Callaghan et al. 1983) as
119 described previously (Yao et al. 2008; Yao et al. 2000). Maximum gradient strength, G_{max},
120 was calibrated to be 57.31 and 55.89 G cm^{-1} for cryoprobes of the 600 MHz and 800 MHz
121 spectrometers, respectively. Spectra were processed using TOPSPIN (Version 3.2, Bruker)
122 and the analyses of diffusion data were initially carried out using the *T_1/T_2 relaxation module*
123 within TOPSPIN (Version 3.2, Bruker) and subsequently performed using *SigmaPlot*
124 (Version 12.5, Systat Software Inc). The translational diffusion coefficient, *D*, was
125 determined by non-linear regression of diffusion weighted intensities or volumes of selected
126 peaks to the following equation:

127 $$I = I_0 \exp\left\{-\gamma^2 s^2 g^2 \delta^2 \left(\Delta - \frac{\delta}{3}\right) D\right\} = I_0 \exp\left(-K^2 D\right) \qquad (1)$$

128 where γ is the proton gyromagnetic ratio and *s*, g, δ and Δ are the shape factor, amplitude,
129 duration and separation of the single pair of gradient pulses, respectively (see Figure 1, and
130 Figures S1a and S1b, Supplementary Materials). For the conventional BPP-STE sequence
131 (Figure S1c), Δ is replaced by (Δ-τ_1/2) with τ_1 being the time interval between the bipolar
132 gradient pulses within the bipolar gradient encoding or decoding segment, set at 200 μs in the
133 present study. The inter-transient and/or inter-increment relaxation delays, excluding the
134 duration of acquisition, were set at 0.2 s for all BEST version sequences in line with delays
135 commonly used in BEST sequences and 2.0 s for the conventional BPP-STE sequence.

136 **Sample preparations**

137 The sample consisting of Val-7 $^{13}C/^{15}N$ double-labelled phosphopeptide
138 (DKE{pTyr}YTVKDDRD) was prepared in 50 mM phosphate buffer (pH 6.8) at 1 mM.
139 After measurements in buffer solution were completed, RNase A was added to the sample to
140 reach an equimolar concentration. The single-residue $^{13}C/^{15}N$ double-labelled phosphopeptide

was obtained from Genscript and RNase A was purchased from Sigma and used without further purification. The B1 immunoglobulin-binding domain of Streptococcal protein (GB1) sample comprised 0.3 mM ^{15}N-labelled GB1 in an imidazole buffer with 50 mM imidazole and 10 mM $CaCl_2$ at pH 6.8. Protocols for the expression and purification of GB1 have been described previously (Sethi et al. 2016). The sample of gramicidin A in SDS micelles was prepared by mixing 10 μL of 50 mM gramicidin A in trifluoroethanol (TFE) with 500 μL of 250 mM SDS solution in 90% H_2O/10% ^2H_2O followed by bath sonication to aid incorporation of the peptide into micelles. The final molar ratio of SDS:gramicidin A was 250:1 with a measured pH of 6.0. Assuming an aggregation number of 62 SDS monomers per micelle, this ensured that the micelles were in molar excess of gramicidin A. Gramicidin A (with ^{15}N labelled Val-7) and SDS (99%) were purchased from CSBio (Menlo Park, USA) and Merck (New Jersey, USA).

Results and discussion

^{1}H-^{15}N HMQC-filtered BEST PFG-NMR Sequence

The pulse sequence of the ^{1}H-^{15}N HMQC-filtered BEST sequence is depicted in Figure 1. It was constructed by appending the diffusion encoding/decoding segment of the standard STE sequence (Tanner 1970), after replacing non-selective hard RF pulses with band-selective shaped-pulses, to the SOFAST-HMQC sequence (Schanda and Brutscher 2005) in a similar fashion as in the ^{13}C-edited 3D BEST-DOSY sequence (Shukla and Dorai 2011). The first and second ^{1}H shaped-pulses are a polychromatic PC9 and r-SNOB as used in the original form of the SOFAST-HMQC sequence, whereas the two shaped-pulses flagged by the translational diffusion encoding/decoding gradient pulses are EBURP-2 and time-reversal EBURP-2, respectively. Durations of each type of shaped pulses were adjusted accordingly

with excitation band-width to match with the spectral region of interest. The 180° ^{13}C-pulse, an adiabatic pulse (Crp60,0.5,20.1) placed in the middle of the indirect chemical shift dimension, is for ^{13}C decoupling when the biomolecules are both ^{15}N and ^{13}C labelled.

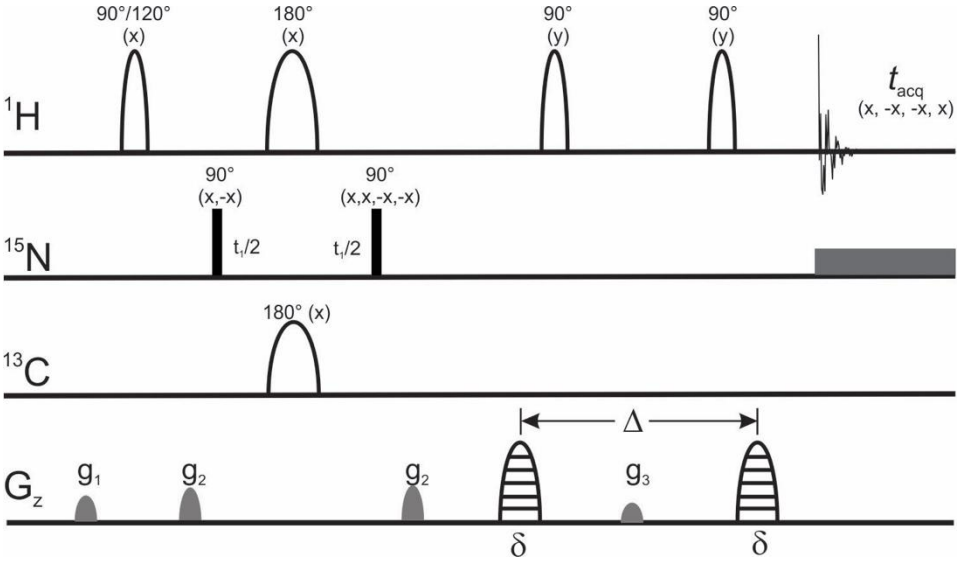

Figure 1 Schematic diagram of ^{1}H-^{15}N HMQC-edited band-selective pulse sequence for measuring translational diffusion coefficients of ^{15}N-labelled peptides and proteins. The sequence is constructed by appending the diffusion encoding/decoding segment of a standard STE sequence to the SOFAST-HMQC sequence (Schanda and Brutscher 2005) in a similar fashion as previously described for 3D ^{13}C BEST-DOSY sequence (Shukla and Dorai 2011). The first ^{1}H excitation pulse, with a flip angle of either 90° or 120°, takes a polychromatic PC9 shape with the second refocusing pulse being an r-SNOB shaped pulse similar as used in the original SOFAST-HMQC sequence (Schanda and Brutscher 2005). The last two shaped 90° pulses flanked by the diffusion encoding and decoding gradients are EBURP-2 and time-reversal EBURP-2 pulses, respectively. Phases for both RF pulses and the receiver are as indicated. Gradients used for the encoding and decoding (marked with horizontal lines) of translational diffusion are sinusoidal-shaped pulses whereas all other (non-stepping) gradients used for coherence selection (HMQC) or artefact suppression (spoiler) are smoothed square pulses (shaded in grey). Durations for g_1, g_2, and g_3 are 1 ms, 1 ms, and 0.6 ms, respectively, with corresponding gradient strengths of 7% G_{max}, 11% G_{max}, and 5% G_{max}. Source code of the sequence for Topspin2.5 and above is available upon request.

Translational diffusion measurement of ^{15}N-labelled peptide in aqueous solution

The ^{1}H-^{15}N HMQC-filtered BEST sequence (Figure 1) for the measurement of translational diffusion coefficients of ^{15}N-labelled biomolecules was first evaluated in aqueous solution using a phosphopeptide (DKE{pTyr}YTVKDDRD) with a single ^{13}C and ^{15}N labelled

residue, Val-7. The diffusion coefficient of the phosphopeptide in phosphate buffer measured at 298 K using the ^{1}H-^{15}N HMQC-filtered BEST sequence (Figure 1) was compared with values determined using alternative sequences (Figure S1, Supplementary Materials), namely (1) ^{1}H-^{13}C HMQC-filtered band-selective sequence, (2) the previously described non-isotope-filtered BEST-STE sequence, and (3) the conventional BPP-STE sequence. The results are summarized in Figure 2. Clearly, the translational diffusion coefficient of the peptide obtained from the new ^{1}H-^{15}N HMQC-filtered BEST sequence (Figure 1) is in excellent agreement with values obtained from all three sequences examined here (Table 1).

As spectral resolution in the heteronuclear (^{15}N or ^{13}C) dimension does not provide additional information for a single residue isotope labelled peptide, only pseudo 2D datasets instead of a complete pseudo 3D dataset were acquired for both ^{1}H-^{15}N HMQC-filtered and ^{1}H-^{13}C HMQC-filtered datasets. A full 3D dataset with the complete acquisition of the ^{15}N chemical shift dimension would provide the resolution needed for resolving potential multiple species in solution in a similar fashion as described previously for the ^{1}H-^{13}C HMQC-edited BEST sequence (Shukla and Dorai 2011).

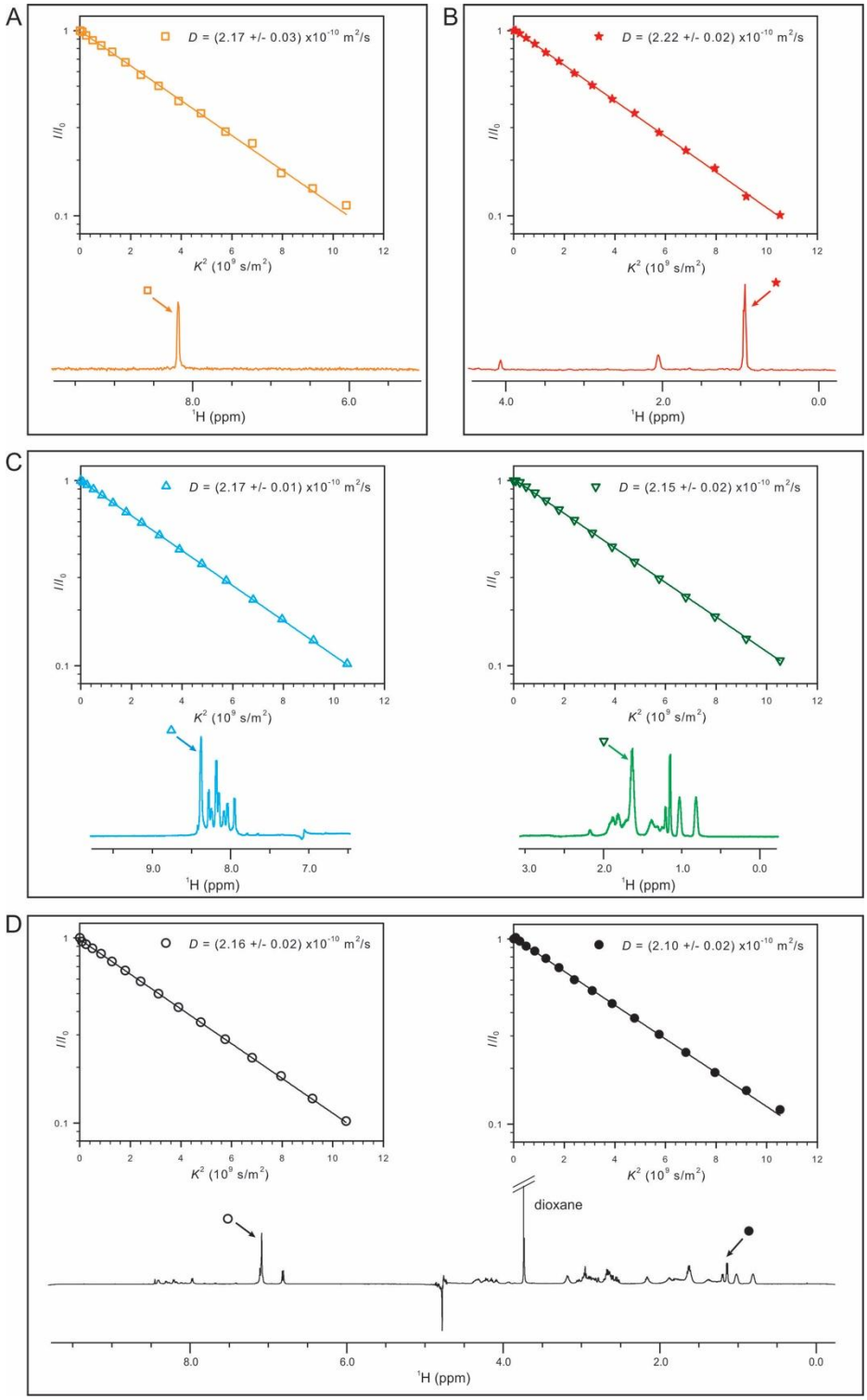

205

206 **Figure 2** Summary of translational diffusion coefficients for a phosphopeptide,
207 DKE{pTyr}YTVKDDRD, with a single-residue (Val-7) labelled with both ^{13}C and ^{15}N in
208 phosphate buffer and pH 6.8, measured at 298.13 K on a Bruker Avance III 600 using PFG-
209 NMR sequences shown in Figure 1 and Figure S1, Supplementary Materials. (A)
210 Translational diffusion induced signal attenuation shown as relative intensity of amide peak
211 arising from $^{13}C/^{15}N$-labelled residue Val-7 versus the strength of diffusion encoding gradient
212 K^2 acquired using ^{1}H-^{15}N HMQC-filtered-edited BEST sequence (Figure 1) together with 1D
213 ^{1}H spectrum at the lowest diffusion-encoding gradient (K^2 = 0.005 x 10^9 sm^{-2}); (B) Similar to

(A) obtained using the ^{1}H-^{13}C HMQC-filtered BEST sequence (Figure S1a, Supplementary Materials); (C) Similar to (A) and (B) obtained using the simple non-filtered BEST-STE sequence (Figure S1b, Supplementary Materials) with the carrier frequency of band-selective pulses centred at the amide (8.4 ppm) and the aliphatic (1.5 ppm) region; (D) Similar data resulting from the conventional non-selective BBP-STE sequence with water suppression achieved using excitation sculpting before acquisition (Figure S1c, Supplementary Materials). Resonances used for the determination of translational diffusion coefficient are indicated in the corresponding diffusion-weighted ^{1}H spectra depicted. For all measurements, a diffusion delay, Δ, of 50 ms and diffusion gradient pulse duration, δ, of 5.0 ms along with a total of 16 steps of gradient encoding, corresponding to K^2 values ranging from 0.005×10^9 sm^{-2} to 10.520×10^9 sm^{-2}, were used.

Translational diffusion measurement of ^{15}N-labelled protein

The application of the ^{1}H-^{15}N HMQC-filtered BEST sequence (Figure 1) to ^{15}N-labelled proteins was also examined. The results obtained for ^{15}N-labelled B1 domain of Streptococcal protein B (GB1) at 298 K are summarized in Figure 3. The pseudo 3D dataset was acquired using 1024 and 64 complex points for the ^{1}H and ^{15}N dimensions, respectively, and with 16 steps (K^2 values ranging from 0.054×10^9 sm^{-2} to 19.44×10^9 sm^{-2}) in the translational diffusion dimension. Diffusion coefficients of GB1 were determined from either individual backbone amide residues or the overall backbone amide profile and the resultant values are in excellent agreement. These measured values are also in excellent agreement with the value measured of resonance (δ= 2.04 ppm) in the aliphatic region using the conventional BPP-STE sequence (Table 1). Notably, the translational diffusion coefficients of proteins or peptides measured using the band-selective excitation sequence are not compromised by the potential presence of amide protons in rapid exchange with solvent water. This was evident by both diffusion coefficients resulting from the analysis of a single residue T11 located in the loop region, which exhibited rapid chemical exchange with solvent water (confirmed by the CLEANEX experiment recorded with a mixing time of 30 ms), and the overall amide profile, including all mobile backbone amides, being able to be fitted satisfactorily to a mono-exponential decay against K^2. Corresponding results for residues T11

and W43 obtained using a non-selective ^{1}H-^{15}N HSQC-edited PFG-NMR sequence (Figure S3, Supplementary Materials) are shown in Figure S2b. The translational diffusion induced signal decay of residue T11 clearly deviated from a single exponential decay due to underlying chemical exchange with solvent. In contrast, the translational diffusion induced signal decay of residue W43 (located within a β-strand and not under rapid exchange with the solvent water) follows a single exponential decay with a resultant translational diffusion coefficient in very good agreement with the value on resonance (δ= 2.04 ppm) in the aliphatic region measured using the conventional BPP-STE sequence.

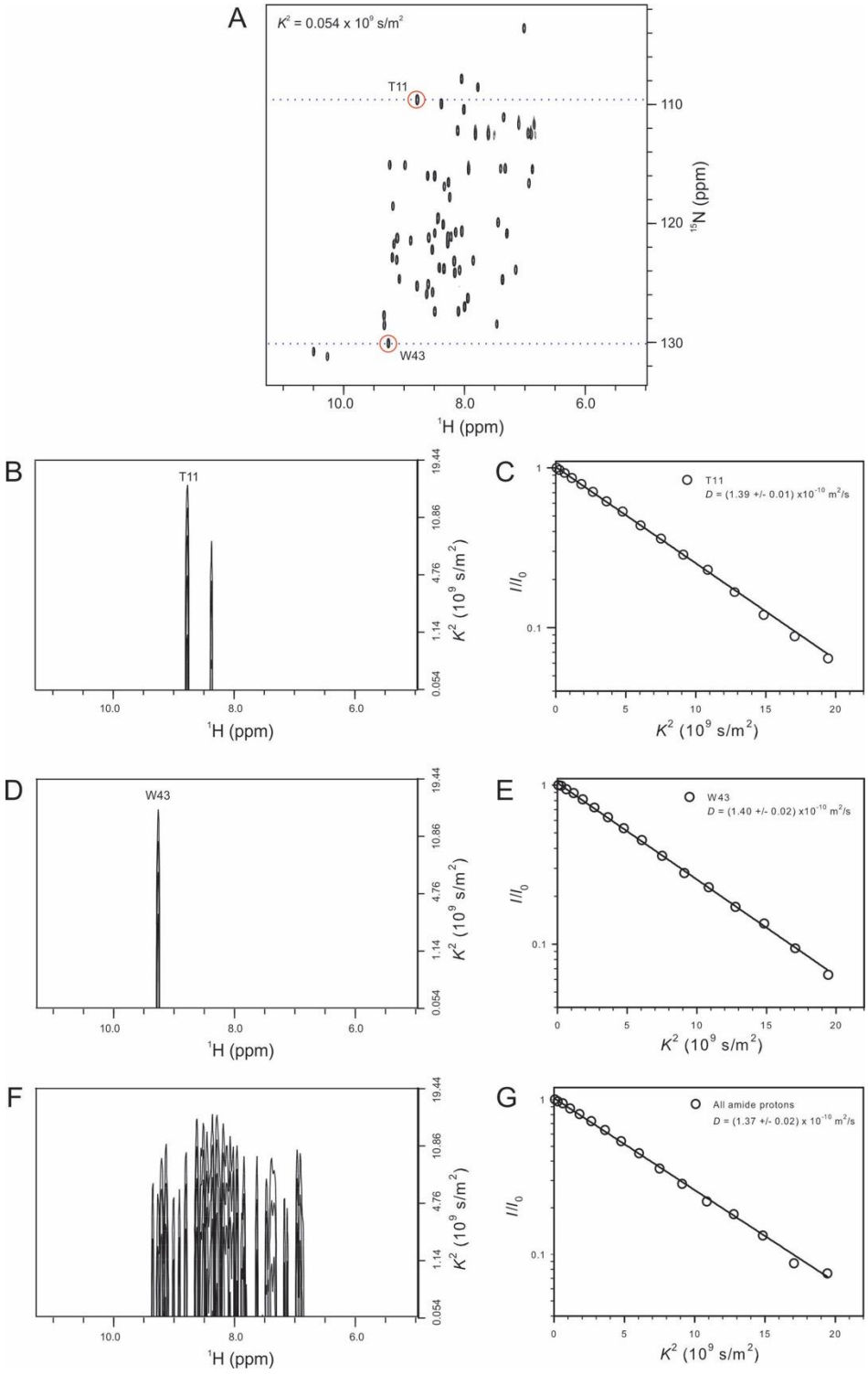

Figure 3 Translational diffusion coefficient of ^{15}N-labelled GB1 measured using the ^{1}H-^{15}N HMQC-filtered BEST sequence (Figure 1) on a Bruker Avance II 800 spectrometer. (A) ^{1}H-^{15}N HMQC spectrum (plane) at the lowest diffusion encoding/decoding value, K^2 = 0.054 x 10^9 sm^{-2}. Backbone amide residues T11 and W43 used in the diffusion analysis are indicated. Assignments were adopted from those reported previously (Barchi et al. 1994). (B, C) showing diffusion plane of residue T11 (located in a loop region which exhibited rapid exchange with solvent water as confirmed by the CLEANEX experiment acquired with a mixing time of 30 ms) and corresponding diffusion induced T11 signal attenuation versus the

strength of diffusion encoding gradient K^2 together with fit to Eq.1. (D, E) Same as (B, C) shown for backbone amide W43 (located within a β-strand and not under rapid exchange with the solvent water). (F, G) 2D Projection along the diffusion dimension and diffusion induced signal attenuation of all backbone amide protons versus the strength of diffusion encoding gradient K^2. Line in (G) represents fit to Eq.1 for the bulk amide signals (integrals from 6.0 to 11.0 ppm). A diffusion delay, Δ, of 50 ms and diffusion gradient pulse duration, δ, of 7.0 ms along with a total of 16 steps of gradient encoding, corresponding to K^2 values ranging from 0.054×10^9 sm^{-2} to 19.44×10^9 sm^{-2}, were used.

A number of non-selective ^{15}N-HSQC/TROSY edited diffusion sequences have been described previously for various applications (Andrec and Prestegard 1997; Buevich and Baum 2002; Horst et al. 2011; Nesmelova et al. 2004; Rajagopalan et al. 2004). The translational diffusion coefficients measured using the band-selective sequences, however, are significantly less likely to be compromised by the presence of solvent exchange of backbone amide protons (Fig. 3F and 3G). Unless translational diffusion-based experiments are applied specifically to probe backbone amide NH exchange where diffusion behaviour of solvent is of interest, the band-selective ^{15}N-filtered sequences, including the one described here, should prove to be superior to the non-selective counterparts for many other types of applications. Such applications could include the filtration of polypeptide and protein signals in complex mixtures (Rajagopalan et al. 2004), the definition of association states of proteins during folding (Buevich and Baum 2002), and direct measurement of biomolecular translational diffusion coefficients in various solution conditions.

Translational diffusion measurement of ^{15}N-labelled peptide in the presence of equimolar unlabelled protein: a model crowed protein solution

The ^{1}H-^{15}N HMQC-filtered BEST sequence has also been applied to measure translational diffusion coefficient of the same phosphopeptide in the presence of equimolar RNase A (1.0 mM). Results obtained from the ^{1}H-^{15}N HMQC-filtered BEST sequence, together with those obtained from the conventional BPP-STE sequence and the ^{1}H-^{13}C HMQC-filtered sequence,

289 are summarised in Figure 4 and the measured apparent translational diffusion coefficients of
290 the phosphopeptide are listed in Table 1. Translational diffusion coefficients of the
291 phosphopeptide measured by both the ^{1}H-^{15}N and ^{1}H-^{13}C HMQC-filtered BEST sequences
292 agree very well (Figure 4a and 4b). Both values are slightly lower than those measured in the
293 absence of RNase A (Figure 2), reflecting an increase of solution viscosity in the presence of
294 RNase A. This is confirmed by a decrease, $D = 0.9 \pm 0.02 \times 10^{-9}$ m^2s^{-1} in the presence of
295 RNase A versus $D = 1.00 \pm 0.02 \times 10^{-9}$ m^2s^{-1} in the absence of RNase A, observed for the
296 measured diffusion coefficients of dioxane in the solution (Figure S4, Supplementary
297 Materials). As evident from Figure 4c and Table 1, in the presence of equimolar unlabelled
298 protein RNase A, direct quantification of the peptide translational diffusion coefficients with
299 the conventional BPP-STE in the absence of isotope-filtering is significantly compromised
300 (Table 1) due to spectral overlap of resonances arising from both the phosphopeptide of
301 interest and the background protein RNase A. Apparent diffusion coefficient determined from
302 peak intensities at a given chemical shift is clearly weighted by resonances contributing to the
303 peak intensities, in the present case, the phosphopeptide and RNase A. Also note that in the
304 lower panel of Figure 4b, aliphatic peaks arising from unlabelled protein RNase A and small
305 molecules, such as dioxane are also visible (peaks marked with x).

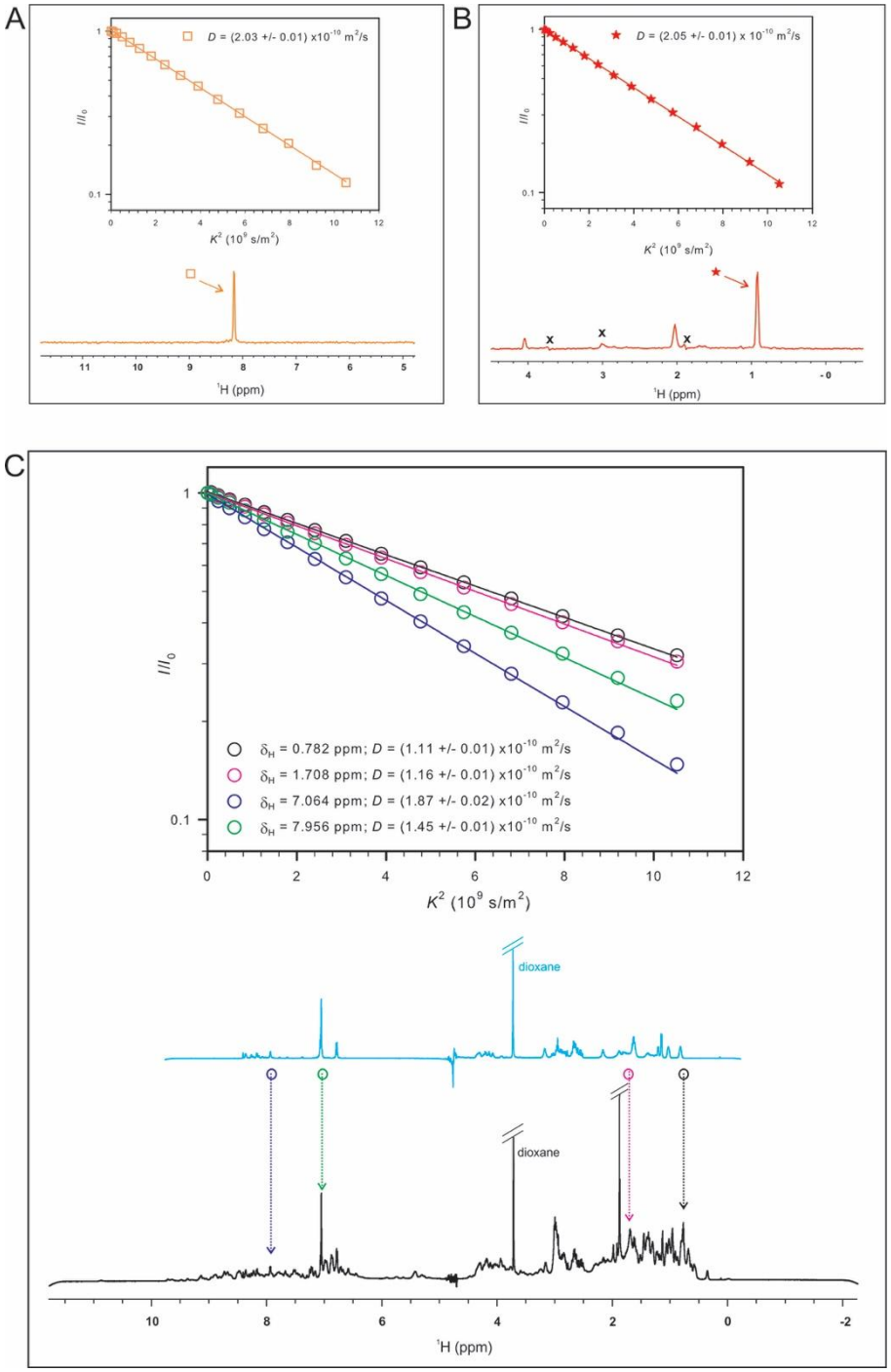

306

307 **Figure 4** Translational diffusion coefficient of the phosphopeptide,
308 DKE{pTyr}YTVKDDRD, in the presence of equimolar RNase A in phosphate buffer, pH
309 6.8, measured at 298.13 K on a Bruker Avance III 600. (A, B) Translational diffusion
310 induced signal attenuation shown as relative intensities of peaks across the spectrum versus
311 the strength of diffusion encoding gradient K^2 acquired using the ^{1}H-^{15}N and ^{1}H-^{13}C HMQC-
312 filtered BEST sequences, respectively. (C) Similar as (A) and (B), obtained using
313 conventional BBP-STE sequence (Figure S1c, Supplementary Materials). The lower panel in
314 (C) displays the full 1D ^{1}H spectrum of the phosphopeptide in the presence of equimolar
315 RNase A (in black) with peaks used for the analysis (upper panel) indicated. Corresponding
316 1D ^{1}H spectrum, acquired with a narrow spectral-width, of phosphopeptide in the absence of

RNase A (in red) is also included for comparison. Same values for Δ, δ, and K^2, as in Figure 2, were used.

Translational diffusion measurement of ^{15}N-labelled membrane peptide in SDS micelles

Translational diffusion coefficients of a single residue (Val-7) ^{15}N-labelled model membrane protein, gramicidin A, in SDS micelles measured with the ^{1}H-^{15}N HMQC-filtered BEST sequence (Figure 1) and the non-isotope-filtered BEST-STE sequence (Figure S1b, Supplementary Materials) are in very good agreement (Figure 5a and 5b, Table 1). Similar results for the SDS micelles measured with the conventional BPP-STE sequence) Figure S1, Supplementary Materials), are shown in Figure 5c and Table 1. The apparent translational diffusion coefficient of SDS micelles (D = 8.67 ± 0.04 x 10^{-11} m^2s^{-1}) is slightly higher than that of gramicidin A (D = 7.24 ± 0.03 x 10^{-11} m^2s^{-1} from BEST-STE and D = 7.36 ± 0.06 x 10^{-11} m^2s^{-1} from ^{1}H-^{15}N HMQC-filtered BEST, respectively) similar as previously reported for Aβ42 peptide in micelles (Yao et al. 2014) and outer membrane protein A (OmpA) in DMPC nanodiscs and Fos-10 detergent micelles (Susac et al. 2014). This observation is consistent with experimentally measured apparent diffusion coefficient of detergent micelles being a weighted average of those with and without protein molecules.

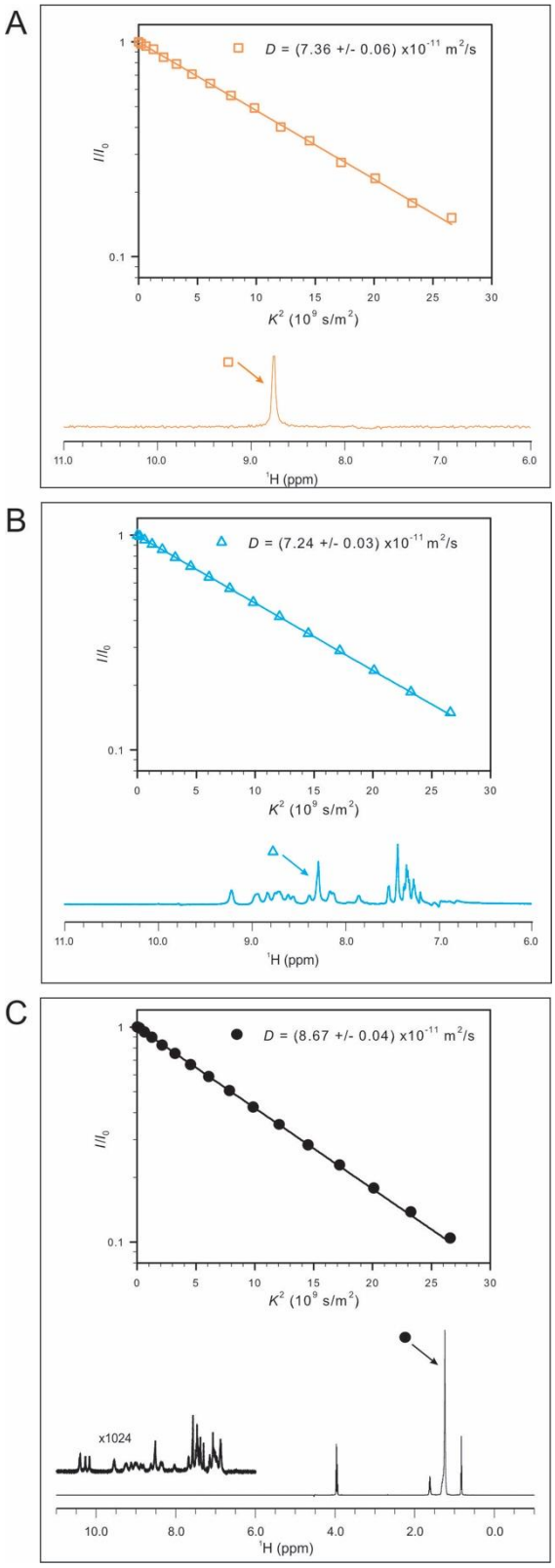

334

335 **Figure 5** Translational diffusion coefficient of single residue (Val-7) ^{15}N labelled membrane
336 peptide, gramicidin A, in SDS micelles at 318.13 K measured on a Bruker Avance III 600.
337 Obtained with: (A) the ^{1}H-^{15}N HMQC-filtered BEST sequence (Figure 1), and (B) the non-
338 filtered BEST sequence (Figure S1b, Supplemental Materials). (C) Corresponding diffusion
339 coefficient of SDS micelles measured using the conventional BPP-LED sequence (Figure

S1c, Supplemental Materials). The inset in (C) displays a partial spectrum of resonances arising from the amide and aromatic protons of gramicidin A after scale-up by a factor of 1024. A diffusion delay, Δ, of 50 ms and diffusion gradient pulse duration, δ, of 8.0 ms along with a total of 16 steps of gradient encoding, corresponding to K^2 values ranging from 0.012×10^9 sm^{-2} to 26.58×10^9 sm^{-2}, were used.

Depending on the average aggregation number for individual detergents, significantly higher molar ratio for the detergent to peptide/protein is usually needed to ensure that the micelles are in excess of the peptide. In our current example, a molar ratio of 250:1 for SDS:gramicidin A was used. Assuming an average aggregation number of 62, this translates into a molar ratio of 4:1 for SDS micelles:gramicidin A. As a result of the molar excess of the detergent, the 1D ^{1}H spectrum is dominated by the signal arising from the SDS (Figure 5C, lower panel). This makes a direct diffusion measurement of the peptide by a conventional PFG-NMR sequence practically impossible unless fully deuterated SDS was to be used. Furthermore, with an SDS to peptide molar ratio of a few hundreds to one, even if the gramicidin A were ^{13}C-labelled, the ^{13}C attached ^{1}H signal arising from the acyl chain of SDS at natural abundance would still dominate the aliphatic region of the ^{1}H spectra, which would hamper application of the ^{1}H-^{13}C HMQC-filtered BEST sequence.

Conclusions

An alternative ^{1}H-^{15}N HMQC-filtered BEST sequence is described in the present report. The sequence takes a simpler form than previously reported BEST-XSTE or SOFAST-XSTE sequence and is readily applicable to NMR spectrometers equipped with probes fitted with a single-axis field gradient, as is the case for most cryoprobes dedicated to bio-NMR. The newly introduced sequence was applied to a number of examples mimicking various solution conditions, including ^{15}N-enriched protein and peptide in aqueous solution, ^{15}N-enriched peptide in the presence of equimolar unlabelled protein, and ^{15}N-enriched membrane peptide

in protonated SDS micelles. Experimentally measured translational diffusion coefficients of protein and peptide under all examined conditions agreed very well with results obtained using existing sequences. This alternative ^{1}H-^{15}N HMQC-filtered sequence provides additional means for the characterization of translational diffusion properties of ^{15}N-enriched proteins and peptides in solution. The sequence should be applicable to use in complex systems (Barhoum et al. 2016), such as protein and ligand complexes (Gossert and Jahnke 2016), protein or peptide in crowded protein solutions (Li et al. 2009; Roosen-Runge et al. 2011; Wang et al. 2010), proteins in detergent micelles – a membrane-mimicking media (Andersson et al. 2004; Chou et al. 2004), and molecules within bicontinuous cubic phases (Eriksson and Lindblom 1993; Larkin et al. 2017; Meikle et al. 2017; Zabara et al. 2017), where use of alternative sequences is hampered due to practical limitations of individual sequences.

Acknowledgments

We thank Dr Aitor Moreno of Bruker for the source code of the ^{1}H-^{15}N HSQC-edited PFG-NMR sequence (Fig. S3, Supplemental Materials).

References

Ali FE, Separovic F, Barrow CJ, Yao SG, Barnham KJ (2006) Copper and zinc mediated oligomerisation of A beta peptides. Int J Pept Res Ther 12:153-164

Altieri AS, Hinton DP, Byrd RA (1995) Association of Biomolecular Systems Via Pulsed-Field Gradient Nmr Self-Diffusion Measurements. J Am Chem Soc 117:7566-7567

Andersson A, Almqvist J, Hagn F, Maler L (2004) Diffusion and dynamics of penetratin in different membrane mimicking media. BBA-Biomembranes 1661:18-25

Andrec M, Prestegard JH (1997) Quantitation of chemical exchange rates using pulsed-field-gradient diffusion measurements. J Biomol NMR 9:136-150

Augustyniak R, Ferrage F, Paquin R, Lequin O, Bodenhausen G (2011) Methods to determine slow diffusion coefficients of biomolecules. Applications to Engrailed 2, a partially disordered protein. J Biomol NMR 50:209-218

Barchi JJ, Grasberger B, Gronenborn AM, Clore GM (1994) Investigation of the Backbone Dynamics of the Igg-Binding Domain of Streptococcal Protein-G by Heteronuclear 2-Dimensional H-1-N-15 Nuclear-Magnetic-Resonance Spectroscopy. Protein Science 3:15-21

Barhoum S, Palit S, Yethiraj A (2016) Diffusion NMR studies of macromolecular complex formation, crowding and confinement in soft materials. Prog Nucl Mag Res Sp 94-95:1-10

Bocian W, Sitkowski J, Tarnowska A, Bednarek E, Kawecki R, Kozminski W, Kozerski L (2008) Direct insight into insulin aggregation by 2D NMR complemented by PFGSE NMR. Proteins 71:1057-1065

Brand T, Cabrita EJ, Morris GA, Gunther R, Hofmann HJ, Berger S (2007) Residue-specific NH exchange rates studied by NMR diffusion experiments. J Magn Reson 187:97-104

Buevich AV, Baum J (2002) Residue-specific real-time NMR diffusion experiments define the association states of proteins during folding. J Am Chem Soc 124:7156-7162

Callaghan PT, Legros MA, Pinder DN (1983) The measurement of diffusion using deuterium pulse field gradient nuclear magnetic resonance J Chem Phys 79:6372-6381

Chou JJ, Baber JL, Bax A (2004) Characterization of phospholipid mixed micelles by translational diffusion. J Biomol NMR 29:299-308

Dehner A, Kessler H (2005) Diffusion NMR spectroscopy: Folding and aggregation of domains in p53. ChemBioChem 6:1550-1565

Didenko T, Boelens R, Rudiger SGD (2011) 3D DOSY-TROSY to determine the translational diffusion coefficient of large protein complexes. Protein Eng Des Sel 24:99-103

Dingley AJ, Mackay JP, Chapman BE, Morris MB, Kuchel PW, Hambly BD, King GF (1995) Measuring protein self-association using pulsed-field-gradient NMR spectroscopy: application to myosin light chain 2. J Biomol NMR 6:321-328

Dyson HJ, Wright PE (2005) Intrinsically unstructured proteins and their functions. Nat Rev Mol Cell Bio 6:197-208

Eriksson PO, Lindblom G (1993) Lipid and Water Diffusion in Bicontinuous Cubic Phases Measured by Nmr. Biophys J 64:129-136

Gossert AD, Jahnke W (2016) NMR in drug discovery: A practical guide to identification and validation of ligands interacting with biological macromolecules. Prog Nucl Mag Res Sp 97:82-125

Horst R, Horwich AL, Wuthrich K (2011) Translational Diffusion of Macromolecular Assemblies Measured Using Transverse-Relaxation-Optimized Pulsed Field Gradient NMR. J Am Chem Soc 133:16354-16357

Jansma AL, Kirkpatrick JP, Hsu AR, Handel TM, Nietlispach D (2010) NMR Analysis of the Structure, Dynamics, and Unique Oligomerization Properties of the Chemokine CCL27. J Biol Chem 285:14424-14437

Larkin TJ, Garvey CJ, Shishmarev D, Kuchel PW, Momot KI (2017) Na+ and solute diffusion in aqueous channels of Myverol bicontinuous cubic phase: PGSE NMR and computer modelling. Magn Reson Chem 55:464-471

Lescop E, Schanda P, Brutscher B (2007) A set of BEST triple-resonance experiments for time-optimized protein resonance assignment. J Magn Reson 187:163-169

Li CG, Wang YQ, Pielak GJ (2009) Translational and Rotational Diffusion of a Small Globular Protein under Crowded Conditions. J Phys Chem B 113:13390-13392

McLachlan GD, Cahill SM, Girvin ME, Almo SC (2007) Acid-induced equilibrium folding intermediate of human platelet profilin. Biochemistry 46:6931-6943

Meikle TG, Yao S, Zabara A, Conn CE, Drummond CJ, Separovic F (2017) Predicting the release profile of small molecules from within the ordered nanostructured lipidic bicontinuous cubic phase using translational diffusion coefficients determined by PFG-NMR. Nanoscale 9:2471-2478

Melnikova DL, Skirda VD, Nesmelova IV (2017) Effect of Intrinsic Disorder and Self-Association on the Translational Diffusion of Proteins: The Case of alpha-Casein. J Phys Chem B 121:2980-2988
Nesmelova IV, Idiyatullin D, Mayo KH (2004) Measuring protein self-diffusion in protein-protein mixtures using a pulsed gradient spin-echo technique with WATERGATE and isotope filtering. J Magn Reson 166:129-133
Price WS (2009) NMR studies of translational motion: Principles and Applications. Cambridge University Press, Cambridge ; New York
Rajagopalan S, Chow C, Raghunathan V, Fry CG, Cavagnero S (2004) NMR spectroscopic filtration of polypeptides and proteins in complex mixtures. J Biomol NMR 29:505-516
Roosen-Runge F, Hennig M, Zhang FJ, Jacobs RMJ, Sztucki M, Schober H, Seydel T, Schreiber F (2011) Protein self-diffusion in crowded solutions. P Natl Acad Sci USA 108:11815-11820
Rothe M, Gruber T, Groger S, Balbach J, Saalwachter K, Roos M (2016) Transient binding accounts for apparent violation of the generalized Stokes-Einstein relation in crowded protein solutions. Phys Chem Chem Phys 18:18006-18014
Schanda P (2009) Fast-pulsing longitudinal relaxation optimized techniques: Enriching the toolbox of fast biomolecular NMR spectroscopy. Prog Nucl Mag Res Sp 55:238-265
Schanda P, Brutscher B (2005) Very fast two-dimensional NMR spectroscopy for real-time investigation of dynamic events in proteins on the time scale of seconds. J Am Chem Soc 127:8014-8015
Sethi A, Bruell S, Patil N, Hossain MA, Scott DJ, Petrie EJ, Bathgate RAD, Gooley PR (2016) The complex binding mode of the peptide hormone H2 relaxin to its receptor RXFP1. Nat Commun 7
Shukla M, Dorai K (2011) Resolving overlaps in diffusion encoded spectra using band-selective pulses in a 3D BEST-DOSY experiment. J Magn Reson 213:69-75
Sillerud LO, Larson RS (2012) Advances in nuclear magnetic resonance for drug discovery. Methods Mol Biol 910:195-266
Stejskal EO, Tanner JE (1965) Spin Diffusion Measurements: Spin Echoes in the Presence of a Time-Dependent Field Gradient. J Chem Phys 42:288-292
Susac L, Horst R, Wuthrich K (2014) Solution- NMR Characterization of Outer- Membrane Protein A from E. coli in Lipid Bilayer Nanodiscs and Detergent Micelles. ChemBioChem 15:995-1000
Tanner JE (1970) Use of Stimulated Echo in Nmr-Diffusion Studies. J Chem Phys 52:2523-&
Wahlstrom A, Cukalevski R, Danielsson J, Jarvet J, Onagi H, Rebek J, Linse S, Graslund A (2012) Specific Binding of a beta-Cyclodextrin Dimer to the Amyloid beta Peptide Modulates the Peptide Aggregation Process. Biochemistry 51:4280-4289
Wang YQ, Benton LA, Singh V, Pielak GJ (2012) Disordered Protein Diffusion under Crowded Conditions. J Phys Chem Lett 3:2703-2706
Wang YQ, Li CG, Pielak GJ (2010) Effects of Proteins on Protein Diffusion. J Am Chem Soc 132:9392-9397
Wu KP, Kim S, Fela DA, Baum J (2008) Characterization of conformational and dynamic properties of natively unfolded human and mouse alpha-synuclein ensembles by NMR: Implication for aggregation. J Mol Biol 378:1104-1115
Yan JL, Kline AD, Mo HP, Zartler ER, Shapiro MJ (2002) Epitope mapping of ligand-receptor interactions by diffusion NMR. J Am Chem Soc 124:9984-9985
Yao S, Babon JJ, Norton RS (2008) Protein effective rotational correlation times from translational self-diffusion coefficients measured by PFG-NMR. Biophys Chem 136:145-151

Yao S, Cherny RA, Bush AI, Masters CL, Barnham KJ (2004) Characterizing bathocuproine self-association and subsequent binding to Alzheimer's disease amyloid beta-peptide by NMR. J Pept Sci 10:210-217

Yao S, Howlett GJ, Norton RS (2000) Peptide self-association in aqueous trifluoroethanol monitored by pulsed field gradient NMR diffusion measurements. J Biomol Nmr 16:109-119

Yao S, Lee EF, Pettikiriarachchi A, Evangelista M, Keizer DW, Fairlie WD (2016) Characterisation of the conformational preference and dynamics of the intrinsically disordered N-terminal region of Beclin 1 by NMR spectroscopy. BBA-Proteins Proteom 1864:1128-1137

Yao S, Weber DK, Separovic F, Keizer DW (2014) Measuring translational diffusion coefficients of peptides and proteins by PFG-NMR using band-selective RF pulses. European Biophysics Journal 43:331-339

Zabara A, Meikle TG, Trenker R, Yao S, Newman J, Peat TS, Separovic F, Conn CE, Call MJ, Call ME, Landau EM, Drummond CJ (2017) Lipidic Cubic Phase-Induced Membrane Protein Crystallization: Interplay Between Lipid Molecular Structure, Mesophase Structure and Properties, and Crystallogenesis. Cryst Growth Des 17:5667-5674

Zhang XC, Perugini MA, Yao S, Adda CG, Murphy VJ, Low A, Anders RF, Norton RS (2008) Solution conformation, backbone dynamics and lipid interactions of the intrinsically unstructured malaria surface protein MSP2. J Mol Biol 379:105-121

519 **Table 1** Comparison of translational diffusion coefficients of biomolecules measured with
520 ^{1}H-^{15}N HMQC-filtered BEST and alternative PFG-NMR sequences

	D (x10^{-10} m^{2}s^{-1})[a]			
	PFG-NMR sequences			
	^{1}H-^{15}N HMQC-BEST	BEST-STE	BPP-STE	^{1}H-^{13}C HMQC-BEST
1, Phosphopeptide in phosphate buffer (298 K)				
	2.17 ± 0.03 (Val-7, 8.16 ppm)	2.10 ± 0.02 (peak, 1.15 ppm)	2.15 ± 0.02 (peak, 1.63 ppm)	2.22 ± 0.02 (Val-7, 0.93 ppm)
		2.16 ± 0.02 (peak, 7.06 ppm)	2.17 ± 0.02 (peak, 8.38 ppm)	
2, GB1 (298 K)				
	1.39 ± 0.01 (Thr-11)		1.44 ± 0.02 (peak, 2.04 ppm)	
	1.40 ± 0.01 (Trp-43)			
	1.37 ± 0.01 (All amides)			
3, Phosphopeptide in equal molar of RNase A (298 K)				
	2.03 ± 0.01 (Val-6, 8.16 ppm)		1.11 ± 0.01 (peak, 0.78 ppm)	2.05 ± 0.01 (Val-6, 0.93 ppm)
			1.16 ± 0.01 (peak, 1.71 ppm)	
			1.87 ± 0.02 (peak, 7.06 ppm)	
			1.45 ± 0.01 (peak, 7.96 ppm)	
4, Gramicidin A in SDS micelles (318 K)				
	0.736 ± 0.006 (Val-7, 8.76 ppm)	0.724 ± 0.003 (peak, 8.28 ppm)		

521 [a] Corresponding diffusion-induced signal decays and non-linear regressions are shown in
522 Figures 2-5 and Figure S2a, Supplementary Materials.